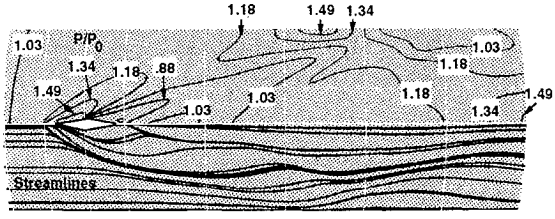

a) 7-deg strut

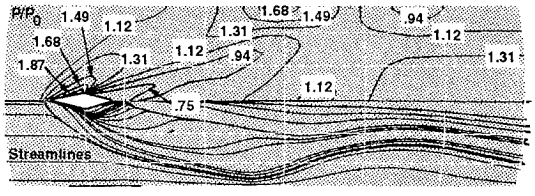

b) 11-deg strut

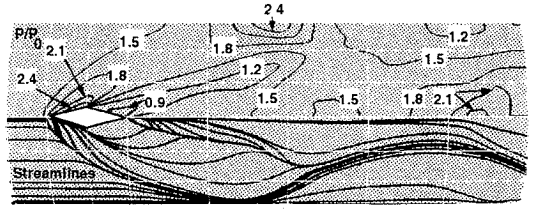

c) 14-deg strut

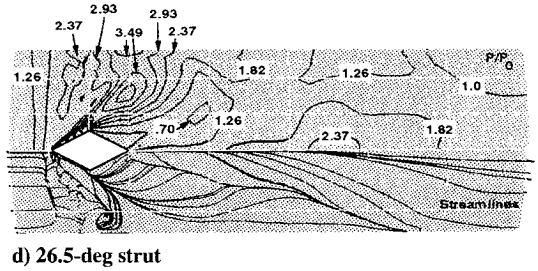

d) 26.5-deg strut

Fig. 3 Centerbody static pressure distributions and limiting streamlines.

Horseshoe vortices formed near the strut leading and trailing edges are each bounded by a coalescense line. The leading-edge vortex entrains boundary-layer fluid; the entrained flow accounts for higher shear stress at the wall under the vortex, as confirmed by oil flow visualization results,[3] and diminishes the flow energy through viscous dissipation. The compression face corner vortex entrains low-energy boundary-layer fluid, which is convected up the strut expansion face toward the duct midplane, and adds low-energy fluid into the strut wake, as illustrated by the total pressure contours in Figs. 1a–1d. In reference to Fig. 1, it can be seen that the leading-edge horseshoe vortex has traveled progressively farther away from the 26.5-deg strut than for the 7- or 14-deg strut cases. For the 26.5-deg strut, this vortex reaches the 45-deg plane of symmetry between struts and lifts off the centerbody surface, as implied by the static pressure distributions and limiting streamline patterns in Fig. 3d. This vortex lift off is associated with a severe separation cell that encompasses the entire width of the flow domain in front of the horseshoe vortex. Large-scale boundary-layer separation is also present on the cowl surface that is not shown here.

Conclusions

A numerical study of supersonic flow about struts of various thicknesses in an annular duct has been conducted. The strut thicknesses evaluated were 0.125, 0.188, 0.25, and 0.5 strut chord lengths that correspond to strut half-angles of 7, 11, 14, and 26.5 deg, respectively. In reference to vortical flow behavior, the compression face corner vortex was observed to migrate up the strut expansion face, away from the centerbody. This behavior is important because this vortex, once downstream of the trailing edge, dominates the viscous wake of the strut. Similar behavior was observed for the corner vortex generated at the cowl–strut intersection. An expansion face vortex has also been identified on the centerbody surface.[3] The formation of a recompression vortex was noted at the trailing edge of the strut. This vortex rotates in the same direction as the leading-edge vortex and is formed by mechanisms similar to those that form the leading-edge vortex.[3] For the strongest interaction studied, the 26.5-deg half-angle strut, these vortices, along with severe boundary-layer separation on the endwalls, dominate the flow. Boundary-layer flow separation with local flow reversal was computed on the cowl surface for the 14-deg strut. These results indicate that, for a core flow Mach number of 3.0, struts of less than 14 deg should be used in flight hardware to ensure unseparated boundary-layer flow.

Acknowledgments

This work was supported by the NASA Lewis Research Center under Contract NAS3-25266 and Grant NAG 3-376. David O. Davis was the project monitor. The computations were performed on the NAS Cray Y-MP at NASA Ames. The authors gratefully acknowledge NASA's support of this research. The assistance of Maryann Johnston is gratefully acknowledged.

References

[1]Stockbridge, R. D., "Experimental Investigation of Shock Wave Boundary-Layer Interactions in an Annular Duct," *Journal of Propulsion and Power*, Vol. 5, No. 3, 1989, pp. 346–352.

[2]Williams, K. E., Gessner, F. B., and Harloff, G. J., "Experimental and Numerical Investigation of Supersonic Turbulent Flow in an Annular Duct," *AIAA Journal*, Vol. 32, No. 7, 1994, pp. 1528–1531; also AIAA Paper 93-3123, July 1993.

[3]Williams, K. E., Harloff, G. J., and Gessner, F. B., "Investigation of Supersonic Flow About Strut/Endwall Intersections in an Annular Duct," *AIAA Journal* (to be published).

[4]Cooper, G. K., and Sirbaugh, J. R., "PARC Code: Theory and Usage," Arnold Engineering Development Center, AEDC-TR-89-15, Arnold AFB, TN, 37389, Dec. 1989.

[5]Baldwin, B. S., and Lomax, H., "Thin Layer Approximation and Algebraic Model for Separated Turbulent Flows," AIAA Paper 78-257, Jan. 1978.

[6]Thomas, P. D., "Numerical Method for Predicting Flow Characteristics and Performance of Nonaxisymmetric Nozzles—Theory," NASA CR 3147, Sept. 1979.

[7]Steinbrenner, J. P., Chawner, J. R., and Fouts, C. L., "The Gridgen 3D Multiple Block Grid Generation System," Wright Patterson Development Center, WRDC-TR-90-3022, Wright Patterson AFB, OH, Vols. 1 and 2, July 1990.

[8]Henderson, T., Huang, W., Lee, K., and Choo, Y., "Three-Dimensional Navier–Stokes Calculation Using Solution Adaptive Grids," AIAA Paper 93-0431, Jan. 1993.

Alleviation of Chattering in Flexible Beam Control via Piezofilm Actuator and Sensor

Seung-Bok Choi*
Inha University, Incheon 402-751, Republic of Korea

Introduction

CONSIDERABLE attention has been focused on the development of smart structures with integrated distributed control

Received Jan. 12, 1994; revision received Nov. 9, 1994; accepted for publication Nov. 9, 1994.

*Assistant Professor, Department of Mechanical Engineering, Smart Structures and Systems Laboratory.

and/or self-monitoring capabilities.[1] These smart structures are employed to control the static and elastodynamic responses of distributed parameter systems operating under variable service conditions. This may be accomplished by tailoring or controlling the mass distribution, the stiffness characteristics, and the energy dissipation characteristics of the structures.

Recently, significant progress has been made in the synthesis of smart structures incorporating piezoelectric films (piezofilms in short). Bailey and Hubbard[2] applied a piezofilm as an active vibration damper for distributed systems. Simulations and experimental investigations on the transient vibration control of a cantilever beam were conducted. They derived two types of controllers based on the Lyapunov stability: a constant-amplitude controller (CAC) and a constant-gain controller (CGC). It has been shown that the CAC is more effective than the CGC with the same maximum voltage. However, when the CAC was employed, undesirable chattering was generated in a settled phase due to excessive supply of control voltages associated with inevitable time delay of hardware systems. This phenomenon has been also observed in the paper studied by Destuynder et al.[3] Research has been also pursued on controlling the dynamic response of articulated machine systems by employing piezofilm actuators and sensors.[4]

In this paper, a hybrid control algorithm that combines the CAC and the CGC is proposed to alleviate undesirable vibration chattering in the settled phase which is the impediment in the successful realization of the CAC. The controller is constructed on the basis of the sign of the tip angular velocity of a cantilever beam as well as the magnitude of the tip deflection. In both the transient and the forced vibration controls, by employing the proposed control algorithm undesirable chattering in the settled phase is completely eliminated or substantially attenuated. Experimental implementations are undertaken to demonstrate these superior control performance characteristics.

Dynamic Modeling

Figure 1 presents the proposed one-dimensional cantilever beam which comprises piezofilms bonded to the top and bottom of the original composite (glass/epoxy) beam. The subscript 1 refers to the original composite beam, and the subscript 2 refers to the piezofilm layer. The governing equation of motion and associated boundary conditions for the proposed system are obtained by considering a conventional Euler–Bernoulli beam model with no internal damping.[2]

They are

$$\frac{\partial^2}{\partial x^2}\left[EI\frac{\partial^2 y(x,t)}{\partial x^2} - c\cdot V(x,t)\right] + \rho A\frac{\partial^2 y(x,t)}{\partial t^2} = F_E(x,t) \tag{1}$$

$$y(x,t) = 0 \quad \text{for } x = 0, \qquad \frac{\partial y(x,t)}{\partial x} = 0 \quad \text{for } x = 0$$

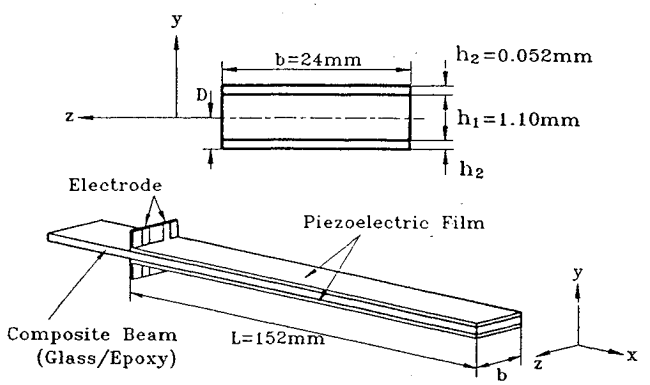

Fig. 1 Schematic diagram of a cantilever beam.

$$EI\frac{\partial^2 y(x,t)}{\partial x^2} = c\cdot V(x,t) \quad \text{for } x = L$$
$$EI\frac{\partial^3 y(x,t)}{\partial x^3} = c\cdot\frac{\partial V(x,t)}{\partial x} \quad \text{for } x = L \tag{2}$$

Here $EI = E_1I_1 + E_2I_2$ and $\rho A = \rho_1A_1 + \rho_2A_2$. $F_E(x,t)$ is the external force, ρ the density of the layer, A the cross-sectional area of the layer, E Young's modulus, I the area moment of inertia, L the beam (or piezofilm) length, and c a constant implying the bending moment associated with the piezofilm strain constant (d_{31}). It is noted that the control voltage $V(x,t)$ may be replaced by $V(t)$ for the proposed piezofilm actuator since it has uniform geometry along its length.

On the other hand, the output voltage $V_f(t)$ produced from the piezofilm sensor is obtained by integrating the electric charge developed at a point on the piezofilm along the entire length of the film surface as follows[5]:

$$V_f(t) = \frac{K_{31}^2\cdot(h_1+2h_2)\cdot b}{2\cdot g_{31}\cdot C}\left.\frac{\partial y(x,t)}{\partial x}\right|_{x=L} \tag{3}$$

Here C is the capacitance of the distributed film sensor, g_{31} the piezoelectric stress constant, and K_{31} the electromechanical coupling factor. It is noted that the output voltage in Eq. (3) represents the angular displacement at the tip of the beam.

Control Algorithm

The impending control issue is to suppress the vibration of the system (1) by employing the control input voltage $V(t)$ to the piezofilm actuator. Bailey and Hubbard[2] employed Lyapunov's second method to formulate control algorithms. This method was chosen because it was simple to drive and an implementable distributed-parameter control law. They proposed a positive definite Lyapunov functional which is basically a measure of the energy in the system. It is given by

$$F = \frac{1}{2}\int_0^L\left[\left(\frac{\partial^2 y(x,t)}{\partial x^2}\right)^2 + \left(\frac{\partial y(x,t)}{\partial t}\right)^2\right]dx \tag{4}$$

Minimizing the time derivative of the functional, vibration control is achieved through bringing the system to an equilibrium state. Therefore, taking the time derivative of Eq. (4) and subsequently substituting Eqs. (1) and (2) into the resultant yields the following two types of control laws: 1) CAC: $V(t) = -K_1\cdot\text{sgn}(c\dot{V}_f)$, and 2) CGC: $V(t) = -K_2\cdot(c\dot{V}_f)$. Here K_1 and K_2 are feedback gains. It has been experimentally verified that the CAC is more effective than the CGC with the same maximum voltage.[2] However, from a practical point of view the CAC causes the structure to produce undesirable chattering in the settled phase. This is attributed to the excessive supply of the control voltage associated with the time delay of the hardware systems. This problem becomes more serious when small vibration levels are considered with a relatively high magnitude of control voltage. On the other hand, the CGC also has some shortcomings in controlling the oscillations in forced vibration. Because of insufficient control forces the suppression efficiency is degraded. This problem becomes more serious when large vibration levels are considered with a relatively small magnitude of control voltage. In this paper, a modified controller is proposed to circumvent these drawbacks. The proposed controller combines the effect of the CAC and the CGC (call it the CAGC, for convenience), and its mathematical expression is given by

$$V(t) = \begin{cases} -K_1\cdot\text{sgn}(c\dot{V}_f), & (V_f)_m > \dfrac{(V_f)_{\max}}{\alpha_1} \\ -K_3\cdot\text{sgn}(c\dot{V}_f), & \dfrac{(V_f)_{\max}}{\alpha_2} < (V_f)_m \leqq \dfrac{(V_f)_{\max}}{\alpha_1} \\ -K_4\cdot(c\dot{V}_f), & (V_f)_m \leqq \dfrac{(V_f)_{\max}}{\alpha_2} \end{cases} \tag{5}$$

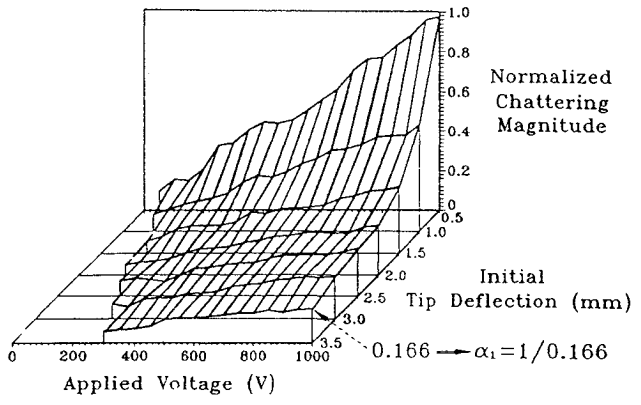

Fig. 2 Determination of switching constant α_1.

where K_i are feedback gains, α_i are switching constants to determine appropriate voltage magnitudes, $(V_f)_{\max}$ represents initial angular amplitude in the absence of control voltage, and $(V_f)_m$ denotes controlled angular amplitude at a certain time.

The determination of the switching constants is the key problem for the control algorithm (5) to be effective. It depends on imposed initial magnitude of the tip deflection and the magnitude of applied maximum feedback voltage in the CAC. Figure 2 briefly shows how to determine the switching constant α_1. For instance, suppose that 3.5 mm of the initial tip deflection is imposed and a $K_1 = 1000$ V in the CAC is chosen. For this case, the switching constant α_1 is equal to the reciprocal of the normalized chattering magnitude (NCM) of 0.166. The NCM was experimentally obtained by normalizing the chattering magnitude at different level of initial deflections and feedback voltages with respect to the chattering magnitude at the level of 0.5 mm and 1000 V. The determination method for the constant α_2 is similar to that for the α_1. As expected, it is clearly observed from Fig. 2 that the chattering magnitude increases as the applied voltage increases for the prescribed initial tip deflection.

Experimental Results and Discussion

The control voltage of the microcomputer was amplified by an amplifier (Trek609A) with a gain of 1000. The controllers were implemented using a personal computer (IBM 386) with a sampling rate of 1000 Hz. The implemented feedback gains K_i and switching constants α_i for $V_{\max} = 1000$ V are as follows: $K_1 = 1000$, $K_2 = 2.6$, $K_3 = 330$, $K_4 = 15$, $\alpha_1 = 6.026$, and $\alpha_2 = 15$.

Figure 3 presents measured transient-vibration control responses. The transient vibrational response characteristics were obtained by exciting the beam with the first-mode natural frequency of 20.0 Hz and subsequently removing this excitation and applying the feedback voltage. It is clearly observed that the CAC is more effective than the CGC but shows unwanted chattering in the settled phase. The chattering was almost eliminated by employing the proposed control algorithm, the CAGC. This implies that the proposed control algorithm produces relatively small adverse control force associated with the time delay in the settled phase, while maintaining a high control effectiveness in the transient phase. The damping factors at 20.0 Hz are distilled by 0.00952, 0.02987, 0.01512, and 0.02659 for the zero voltage, CAC, CGC, and CAGC, respectively.

Figure 4 presents measured forced vibration control responses. The forced vibrational responses were generated by exciting the beam with the first natural frequency of 20.0 Hz and control algorithms applied. It is evident from this figure that the CGC is insufficient to suppress the imposed magnitude of oscillation, whereas the CAC is effective except for the occurrence of chattering in the settled phase. The magnitude of the chattering was substantially reduced by employing the proposed control algorithm. The damping factors for the CAC and CGAC are distilled by 0.02910 and

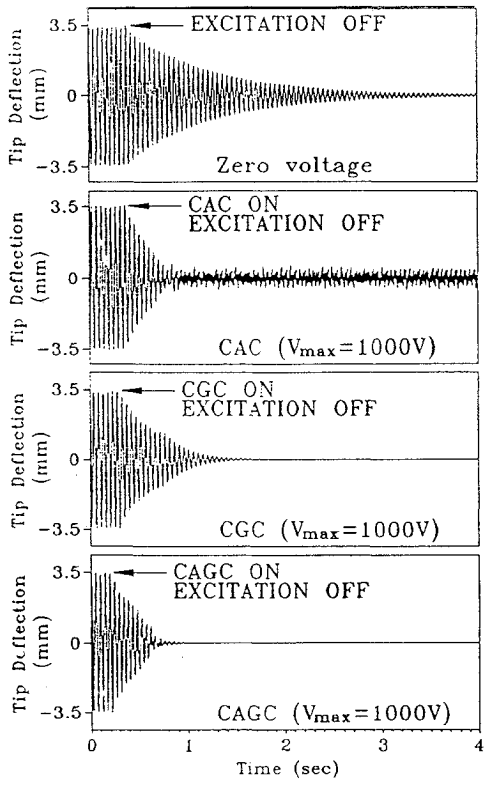

Fig. 3 Transient vibration control responses.

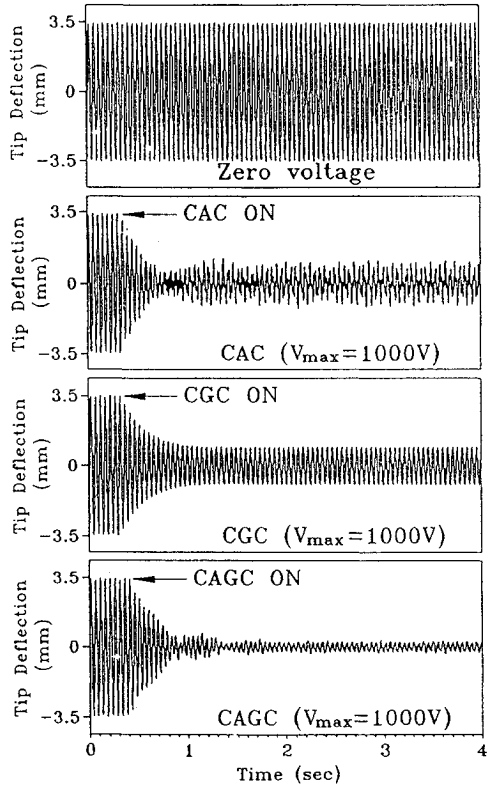

Fig. 4 Forced vibration control responses.

0.02646, respectively. However, the smaller time delay of the experimental hardware is still required to improve control performances especially in the settled phase.

The experimental results presented in this study indicate that the application of an appropriate magnitude of control voltage with respect to the oscillation magnitude and also the employment of

high-resolution hardware systems may improve the control performances of distributed parameter systems featuring piezofilm actuators and sensors.

References

[1]Gandhi, M. V., and Thompson, B. S., *Smart Materials and Structures*, Chap. 3, Chapman and Hall, London, 1992, Chap. 3.

[2]Bailey, T., and Hubbard, J. E., Jr., "Distributed Piezoelectric-Polymer Active Vibration Control of a Cantilever Beam," *Journal of Guidance, Control, and Dynamics*, Vol. 8, No. 5, 1985, pp. 605–611.

[3]Destuynder, P., Legrain, I., Castel, L., and Richard, N., "Piezoelectric Wafers for Reducing the Structure Vibrations," *Intelligent Structural Systems*, edited by H. S. Tzou and G. L. Anderson, Kluwer Academic, Norwell, MA, 1992, pp. 243–284.

[4]Choi, S. B., Cheong, C. C., Thompson, B. S., and Gandhi, M. V., "Vibration Control of Flexible Linkage Mechanisms Using Piezoelectric Films," *Mechanism and Machine Theory*, Vol. 29, No. 4, 1994, pp. 535–546.

[5]Hubbard, J. E., Jr., "Distributed Sensors and Actuators for Vibration Control in Elastic Components," *NOISE-CON87 Proceedings of Noise Conference*, State College, PA, 1987, pp. 407–412.

Errata

Diverging Solutions of the Boundary-Layer Equations near a Plane of Symmetry

Hans Thomann
Swiss Federal Institute of Technology, 8092 Zürich, Switzerland

[AIAA Journal 32 (9), pp. 1923–1925 (1994)]

BECAUSE of an error in the production process, the expression for $w_z(x)$ at the top of page 1923 appeared incorrectly. It should read

$$w_z(x) = A \cdot \exp[-(x - x_0)^2/B]$$

AIAA regrets this error.